J Therm Anal Calorim (2012) 109:663–669
DOI 10.1007/s10973-012-2372-9

Pore size distribution of micelle-templated silicas studied by thermoporosimetry using water and *n*-heptane

Dorota Majda · Wacław Makowski · Maria Mańko

Bretsznajder Special Chapter

Abstract Thermoporosimetry, i.e., DSC measurements of melting point depression of water and heptane confined in mesopores, has been used for determination the pore size distribution of several mesoporous silicas synthesized with the use of micelle templates. Porosity of these materials was additionally characterized by low-temperature nitrogen adsorption and quasi-equilibrated thermodesorption of nonane. The pore size distributions obtained using the water thermoporosimetry were similar to those determined using the other methods, but the pore size values found for the narrow pore materials were underestimated by ca 1 nm. Too large pore sizes obtained for the wide pore silica from heptane thermoporosimetry were attributed to nonlinear dependence of the melting point depression on the reciprocal of the pore size.

Keywords Thermoporosimetry · DSC · Mesoporous silica · Pore size distribution

Introduction

Nanostructured materials have attracted substantial interest in many fields of science because of their potential application [1]. Among them the ordered mesoporous silicas, such as MCM-41 or SBA-15, exhibiting well-ordered structures which can be controlled during synthesis, are ones of the most promising [2]. A thorough understanding the properties of porous materials requires specific methods of characterization, especially concerning their porosity. In general, the applied techniques may be divided into four main categories: microscopy, X-ray scattering, liquid intrusion and gas adsorption techniques. The most popular method is based on measurements of the low temperature adsorption isotherms of nitrogen or argon [3, 4]. It is well established but has also some disadvantages.

Gas adsorption porosimetry, operating on the principle of the micropore filling and capillary condensation in the mesopores, necessitates an understanding of the properties of the liquid phase confined inside the pores, which may be different from those of liquid adsorbate under standard conditions. However, in the methods based on the Kelvin equation, no influence of the pore curvature on the properties of the adsorbed phase is taken into consideration [5]. The desorption isotherm used in determination of the pore size distribution (PSD) is affected by the pore network: when pressure is reduced, liquid will evaporate from large open pores, but pores of the same size that are connected to the surface with narrower channels remain filled [6]. This changes the shape of the PSD. Despite the fact that this method has been used for decades, there are still some other effects that are not properly understood, e.g., hysteresis phenomena [7–9].

Long time of sample preparation and measurements, especially in case of nitrogen, expensive equipment, relatively large amounts of samples needed and limited choice of the adsorptives are the main drawbacks of the gas adsorption porosimetry. A novel adsorption method for studying meso- and micropore materials which is free from some of those limitations is a quasi-equilibrated temperature-programmed desorption and adsorption (QE-TPDA) of volatile hydrocarbons [10–13]. The QE-TPDA of

Electronic supplementary material The online version of this article (doi:10.1007/s10973-012-2372-9) contains supplementary material, which is available to authorized users.

D. Majda (✉) · W. Makowski · M. Mańko
Department of Chemistry, Jagiellonian University, Ingardena 3, 30-060 Krakow, Poland
e-mail: majda@chemia.uj.edu.pl

n-nonane allows determination of the mesopore size distributions as well as the micro- and mesopore volumes [13]. Main advantages of this technique are: relatively short time of the measurements (2–4 h), simple and inexpensive equipment, small samples required (5–10 mg) and possibility of performing cyclic measurements combined with modification of the studied sample.

Thermoporosimetry (TPM), also known as thermoporometry, is another method, allowing characterization of mesoporous materials [3]. It has been known since works of Thomson [14, 15] that a fluid confined in the pores of a material experiences an important shift of its liquid to solid transition temperature. It has also been observed that this shift is related to the size of the pore, in which the liquid is trapped [15].

A liquid to solid phase transition requires formation of crystallization nuclei. In fact, such a nucleus must reach a critical radius, which allows it to start the growth of the solid phase. This critical radius is related to temperature: the smaller the size of the nucleus, the lower the temperature. Inside the divided medium the critical nucleus radius cannot be higher than the size of the cavity in which the liquid is trapped. Consequently, to crystallize the confined liquid, it is necessary to decrease the temperature in order to reach the value corresponding to the pore size. Thus, the freezing point depression observed for the trapped liquid can be related to the size of the pore it is possible to calculate the PSD of the medium under study. This idea is the basis of the TPM, derived by Brun at el. [16, 17]. Application of this technique is very simple, fast, inexpensive, and usually nondestructive. Soaking the porous material in the liquid and measuring the melting or crystallization temperature by differential scanning calorimetry (DSC) is enough to perform pore characterization.

Despite the simplicity and versatility of the DSC porosimetry, so far this method has been rarely used for routine characterization of the porous materials and the reference literature data are scarce, especially for liquids other than water. One of the first reports of application DSC to study the porosity of MCM-41 molecular sieves with various pore diameters was presented by Kloetstra et al. [18]. Using water as the confined liquid, the authors obtained the results that stayed in a very good agreement with the nitrogen physisorption data. The accuracy of water TPM applied for the characterization of SBA-15 was examined by Yamamoto et al. [19]. Again the porous properties evaluated by TPM fitted well with the results of Ar gas adsorption method.

Water was historically first and still remains the most common probe liquid, which is relevant especially for examining materials and coatings designed specifically to absorb aqueous solutions. Another advantage to using water is that its heat of fusion, $\Delta H_m = 334$ J/g, is up to an order of magnitude larger than most organic liquids. The large ΔH_m of water enhances the sensitivity of the DSC technique and allows decreasing size of the studied samples [3]. However, in addition to water, several organic liquids, such as benzene [16], heptane [20], cyclohexane [21], acetonitrile [22], chlorobenzene, or 1.4 dioxane [4] have been also used in TPM. They are of interest because of their varying degrees of polarity and hydrophobicity that may reveal differences in surface chemistry of the porous materials.

The aim of this study was a complementary study on porosity of several model mesoporous materials using different experimental techniques. DSC measurements of the melting point depression of water and *n*-heptane were applied for porosity characterization of four micelle-templated mesoporous silicas: SBA-15, MCM-41, MCM-41/TMB, and HMS, differing in the pore size. The TPM PSDs were compared with those obtained from N_2 adsorption isotherms and from QE-TPDA profiles of *n*-nonane.

Experimental

Ordered mesoporous siliceous materials were prepared in the presence of long-chain quaternary ammonium cations with or without addition of 1.3.5-trimethylbenzene (MCM-41/TMB and MCM-41, respectivly) hexadecyltrimethylamine (HMS) or triblock copolymer (SBA-15) as surfactants.

The MCM-41 synthesis was carried out at 50 °C. Firstly 0.36 g of sodium hydroxide (Carlo Erba) was dissolved in 19.19 g of deionized water. Then, 1.21 g of a cationic surfactant, hexadecyltrimethylammonium bromide (98 % CTAB, Sigma-Aldrich) were added in the alkali solution. After dissolution, 2.0 g of pyrogenic silica (Aerosil 200 V, Degussa) were gradually added to the solution. The final suspension was stirred for 1 h. A hydrothermal treatment of the obtained gel was carried out in a stainless steel autoclave for 2 weeks at 115 °C. The solid was filtered, washed with deionized water until neutral pH and dried overnight at 80 °C [23].

The synthesis of MCM-41/TMB was performed at 50 °C. Firstly the alkali solution was prepared by mixing 0.89 g of sodium hydroxide (Carlo Erba) with 47.97 g of deionized water. After dissolution, 3.02 g of hexadecyltrimethyl ammonium bromide (98 % CTAB, Sigma-Aldrich) and 13.11 g of 1.3.5-trimethylbenzene (TMB, Aldrich) were added. When a homogenous mixture was obtained, 5.0 g of the pyrogenic silica (Aerosil 200 V, Degussa) were gradually added and the suspension was stirred for 30 min. The obtained gel was hydrothermally treated in a stainless steel autoclave for 24 h at 115 °C. The solid was filtered, washed with deionized water until neutral pH and dried during 2 weeks at 115 °C [24].

SBA-15 was synthesized by dissolving 3.91 g of a triblock copolymer of ethylene and propylene oxide (Pluronic P123, Aldrich) in 99.31 g of deionized water and 21.0 g of hydrochloric acid (37 %, Aldrich), at 55 °C. When the polymer was totally dissolved 9.45 g of tetraethyl orthosilicate (TEOS, Aldrich) were added and the final solution was stirred during 5 h. The resulting gel was aged in a teflon-lined stainless steel autoclave at 60 °C for 24 h. The obtained solid was filtered, washed with deionized water until neutral pH and dried overnight at 80 °C [23].

The preparation of HMS was carried out at the ambient temperature. First, 32.25 g of absolute ethanol (Aldrich) was mixed with 64.85 g of deionized water and 6.04 g of hexadecylamine (90 %, Aldrich). After 3 h of dissolution, a 20.84 g of TEOS was added and the solution was stirred for 1 h. The mixture was aged during 24 h without agitation. The solid was filtered and dried for 24 h at 80 °C [25].

All synthesized materials were calcined in air flow for 8 h at 550 °C with a temperature ramp of 2 °C/min. White powders were obtained. The presence of well-ordered mesopores in the calcined silicas MCM-41, HMS and SBA-15 was confirmed by the low-angle X-ray diffraction (supplementary materials).

The N_2 adsorption–desorption isotherms were measured at −196 °C on a Micromeritics TriStar 3000 apparatus. Prior the each measurement, the sample was outgassed in vacuum at 250 °C for 12 h. The apparent surface areas were determined according to the BET model from the adsorption branch. Average pore diameters have been evaluated from the nitrogen desorption branch according to the Broekhoff and De Boer (BdB) method. The mesopore size distributions were calculated from the desorption branch using the classical BJH scheme [26] as well as an improved Kruk–Jaroniec–Sayari model (KJSi, [27]). The latter approach, utilizing instead the Kelvin equation an empirical function with fitted parameters for quantification of the pore size vs. partial pressure relation, gives for the micelle-templated silicas the pores size distributions that are in very good agreement with those computed using NL-DFT method.

The QE-TPDA experiments were performed using a temperature-programmed desorption system equipped with a gas chromatographic thermal conductivity detector (GC TCD Valco Microvolume). A small sample of the calcined porous silica (about 2–4 mg) was placed in a quartz tube (OD 6 mm, 15 cm long) connected to the detector, between two quartz wool plugs. Helium (5.0, Air Products) was used as a carrier gas. In this system, there were two independent carrier gas lines controlled by mass flow controllers (Brooks). One of these lines was equipped with a saturator continuously adding a small admixture of nonane to the stream of He. Using a 4-port switching valve the composition of the gas flowing through the sample could be easily changed from pure He to He containing about 0.4 % of nonane. The lines were heated in order to avoid any condensation or adsorption of nonane vapor on tubing. Prior the QE-TPDA measurements each sample was activated by heating in the flow of He to 500 °C at 10 °C/min and cooled down to the room temperature. Then He was replaced by the He/nonane mixture, flowing through the sample tube with the same flow rate. The QE-TPDA measurements were performed by heating the sample with the pre-adsorbed nonane in the flow of He/nonane mixture (8 cm^3/min) according to a temperature program consisting of several heating and cooling ramps (with the heating and cooling rates of 1 or 2 °C/min).

The DSC measurements were performed using Mettler Toledo apparatus: DSC 821^e equipped with intracooler unit which allows a scanning range of temperature between −60 and +600 °C when water was used as a probe liquid and DSC 822^e equipped with a liquid nitrogen cooling system allowing work between −150 and +400 °C for *n*-heptane measurements. Calibration for heat flux and temperature was done with an indium and zinc metal standards. Pore diameters are determined from the melting point depression, relative to the excess phase, so that each experiment was internally calibrated for temperature [4]. Samples of about 4 mg were placed in aluminum pans and heated to 400 °C in order to empty the pores. After cooling to the room temperature two drops of the solvent were added to maintain the sample in an excess of liquid. To avoid super-cooling effect the samples were quenched far below the equilibrium freezing temperature. Thermoporometry measurements on frozen samples were done only in a heating mode, with the heating rate $\beta = 1$ or 2 °C/min. After the TMP experiments a small hole was made in the crucible's lid and the sample was heated up to 400 °C to evaporate the liquid component in order to determine its mass.

Results and discussion

The low temperature isotherms of N_2 adsorption and the quasi-equilibrated thermodesorption profiles of nonane shown in Fig. 1, confirm mesoporosity of the studied silicas.

All the parameters calculated from these results (Table 1) are in agreement with the expected properties of theses materials. The pore size increases is series MCM-41, HMS, SBA-15 to MCM-41/TBM, as indicated by the increasing pressure corresponding to the capillary condensation step in the adsorption isotherms and decreasing temperature of the thermodesorption peaks. Differences in the pore volume are reflected by different adsorption value close to the saturation pressure and different intensities of

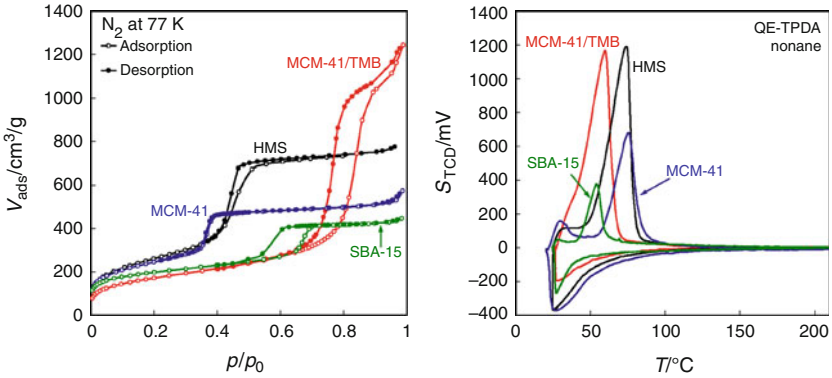

Fig. 1 Porosity characterization of the studied silicas by low temperature adsorption of N_2 and QE-TPDA of nonane

Table 1 Characterization parameters for studied materials measured by nitrogen adsorption and QE-TPDA of nonane

Material	N_2				nC_9
	D_{BdB} (nm)	S_{BET} (m^2/g)	V_{micro} (cm^3/g)	V_{tot} (cm^3/g)	V_{tot} (cm^3/g)
MCM-41	3.7	879	0.03	0.79	0.86
HMS	4.4	955	0.00	1.15	0.72
SBA-15	6.0	720	0.07	0.66	0.51
MCM-41/TMB	11.2	626	0.01	1.93	1.75

the thermodesorption peaks. Analysis of the adsorption isotherms and QE-TPDA profiles showed negligible microporosity of these materials.

DSC curves for water and for *n*-heptane are plotted in the Fig. 2. The first endothermic peaks correspond to the melting of the solid confined in the pores while the second ones result from the melting of the probe outside the pores.

The differences between the melting temperatures for studied samples were as follow: for MCM-41 $\Delta T = 36$ °C in case of water and 47 °C in case of *n*-heptane. For HMS it was 27 °C for water and 38 °C for *n*-heptane. The temperature depression observed for SBA-15 was 15 and 22 °C for water and *n*-heptane, respectively, and for MCM-41/TMB ΔT was equal to 6 °C for water and 9 °C for the alkane. Small pores produce a large temperature depression. The TPM curves for both liquids show the same tendency in the pore size as it was observed by nitrogen adsorption and QE-TPDA of nonane.

According to the Gibbs–Thomson equation the observed shift of the melting point of a solid confined in the pores can by written:

$$\Delta T = T - T_0 = -\frac{\gamma_{ls} T_0}{\rho \Delta h}\frac{dA}{dV} = -K\frac{dA}{dV} \quad (1)$$

where ΔT is the melting point depression, T_0 is the bulk melting temperature, γ_{ls} is the surface tension of liquid–solid interface, ρ is the density, h is the specific enthalpy of melting, and dA/dV is the curvature of the solid–liquid

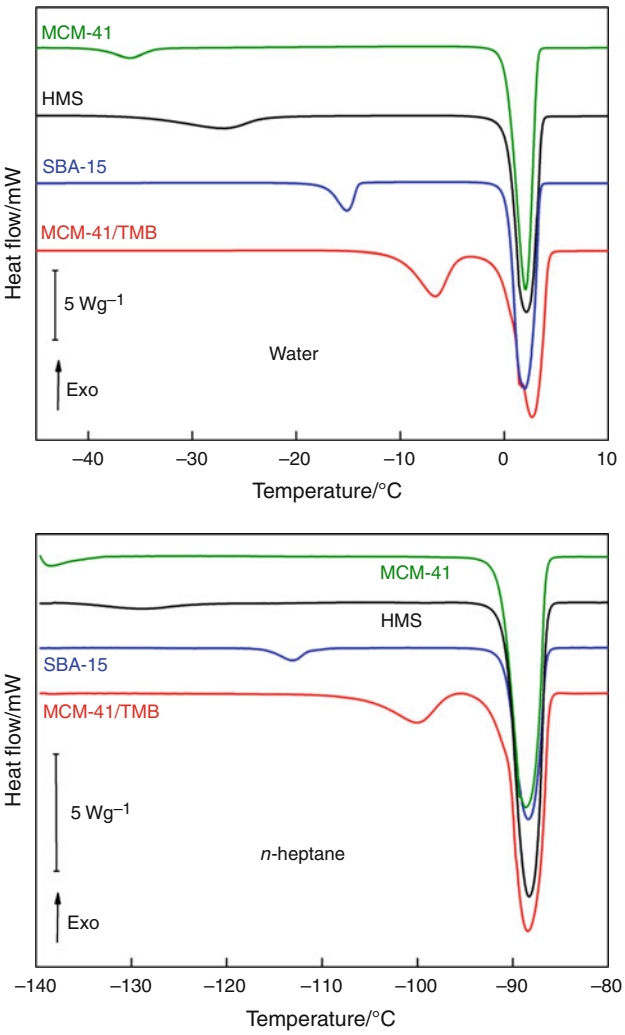

Fig. 2 DSC curves of water and *n*-heptane confined in the studied silica

interface which is $1/r$ for cylinder and $2/r$ for sphere, where r is the radius of the curvature [28]. According to this equation, the shift of the transition temperature of a confined liquid is inversely proportional to the radius of the pore in which it is confined. In fact it is well known that not

all the solvent takes part in the phase transition and that a significant part of it adsorbed on the surface of the pore remains liquid. Consequently, the radius measured by application of the Gibbs–Thomson equation should be written as $R = R_p - t$, where t is the thickness of the non-freezing liquid layer. This leads to the final equation:

$$R_p = \frac{K}{\Delta T} + t. \quad (2)$$

A serious drawback in the TPM technique lies in the fact that the physical parameters, such as surface tension, heat of fusion and density must be known a priori. Also the temperature dependencies on these parameters should be known in the temperature range of the experiment. This is challenging if not impossible to determine them indepen dently. Thus, the experimental work often resorts to the use of reference materials with known pore size for calibration procedure that takes into account also the thickness of non-freezing liquid layer. Since the TPM attracts more and more attention, correlation between pore radius and melting depression temperature, obtained from fitting a polynomial to the calibration data, for various liquids can be found in the literature [4, 16, 17, 22, 29–33]. It is not entirely clear why the equations for the same liquid obtained by various groups differ from each other. Probably the reason is that they were not obtained by the same manner and the materials taken for calibration were also different, especially in the range of pore radii. Another reason can come from the fact that not all authors follow the same assumptions.

To transform TPM result into PSD the temperature axis must be converted into a pore size scale and the heat flow output into a differential pore volume. The basis for relating temperature to pore radius is through the Gibbs–Thompson or through empirical equation.

After a baseline subtraction step that effectively removes the underlying heat capacity contribution to the DSC signal, the heat flow curve, dQ/dt, is converted to dV_p/dR_p according to the equation:

$$\frac{dV_p}{dR_p} = \frac{dQ}{dt}\frac{dt}{d(\Delta T)}\frac{d(\Delta T)}{dR_p}\frac{1}{m\Delta H_f \rho} \quad (3)$$

where $d(\Delta T)/dt$ is the scanning rate of the DSC experiment, m is the mass of dry porous material, and ΔH_f and ρ are the heat of fusion and density for the probe fluid, respectively. The quantity $d(\Delta T)/dR_p$ is determined from an empirical expression. The density taken into the calculations is the density of the adsorbate at the start of the measurement, i.e., solid density for a heating experiment.

For interpretation the results obtained in present work the following value were used: $\Delta H_f = 334$ J/g, $\rho_{ice} = 0.917 \cdot (1.032 - 1.17 \times 10^{-4} T)$ g/cm^3 for water [4, 32] and $\Delta H_f = 140$ J/g, $\rho = 0.684$ g/cm^3 for n-heptane.

For water TPM the temperature axis were converted into a pore size scale through the empirical equation given by Landry [4]:

$$R_p(\text{nm}) = \frac{19.082}{\Delta T + 0.1207} + 1.12 \quad (4)$$

This relation was derived assuming no linearity between ΔT and $1/R_p$.

For TPM study based on melting of n-heptane the equation proposed by Nedelec et al. [29] was used. According to our best knowledge, this is the only one that can be found in the literature:

$$R_p(\text{nm}) = \frac{58.74}{\Delta T} + 0.24. \quad (5)$$

The PSD of studied materials obtained by means of TPM, together with the PSDs calculated form of the N_2 desorption isotherms and QE-TPDA profiles are plotted in Fig. 3. Values of the parameters characterizing porosity based on the TPM results are listed in Table 2, in comparison with the corresponding data found using the other methods.

The TPM-based pores size distributions are generally similar to those determined by the other methods. However, the mesopore sizes obtained for the narrow pore materials (MCM-41 and HMS) are closer to the corresponding values found in the N_2-BJH and nonane QE-TPDA PSDs, than to the more accurate data obtained from the KJSi model. For the wide pore silicas the pore sizes derived from the H_2O TPM and nonane QE-TPDA PSDs remain lower than the KJSi values, but those obtained from heptane TPM are almost the same (for SBA-15) or much larger (for MCM-41/TMB).

It should be pointed out that the intensity of all PSD peaks based on the TPM measurements are lower in comparison to these obtained from the other methods. An important reason of this fact seems to lie in differences in calculations of the pore volume in the TPM method comparing to the models used for interpretation N_2 adsorption isotherms and QE-TPDA profiles. In the latter approach thickness of the film adsorbed on the walls of the emptied pores is quantified and its volume is accounted for. On contrary, in the TPM calculations of the PSD volume of the nonfreezing layer was not taken into account. Therefore, the values of the pore volume corresponding to the integral intensity of the TPM PSD peaks shown in Table 2 are about 30 % of the pore volume calculated from N_2 adsorption data.

However, the equations relating depression of the melting point with the pore size (Eqs. 4 and 5) contain correction corresponding to thickness of this layer, therefore positions of the peaks in the TPM PDSs are more correct, with exception of the heptane TPM PSDs for SBA-15 and

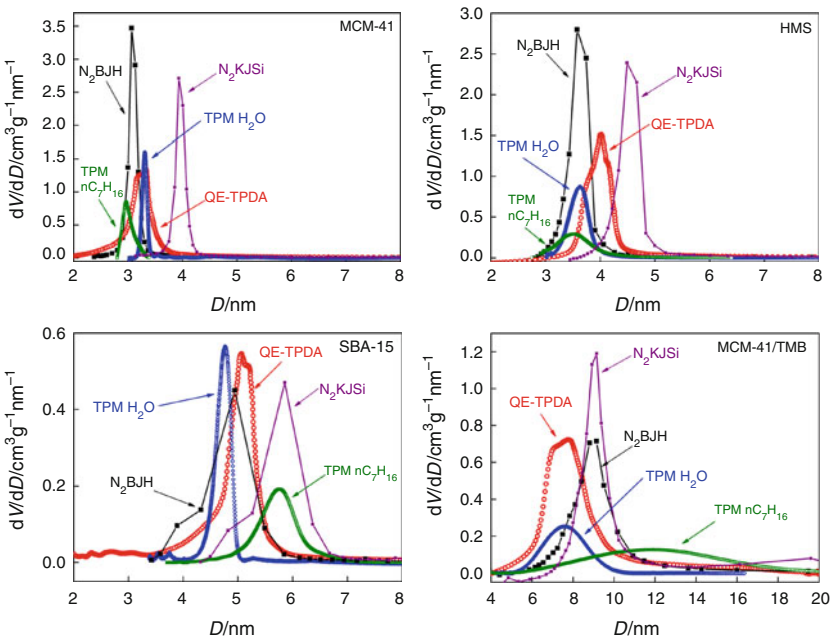

Fig. 3 Comparison of the PSD studied by TPM, N_2 ads and QE-TPDA of nonane

Table 2 Values of the mesopore size and volume calculated using TPM compared with data obtained using the other methods

Material	D_{PSD} (nm)					V_{TPM} (cm^3/g)		V_{TPM}/V_{N2} (%)	
	N_2		QE-TPDA	TPM_{H2O}	TPM_{nC7}	H_2O	nC7	H_2O	nC7
	BJH	KJSi							
MCM-41	3.1	3.9	3.3	3.3	3.0	0.19	0.22	24	28
HMS	3.6	4.5	4.0	3.6	3.5	0.41	0.24	36	20
SBA-15	4.9	5.8	5.1	4.8	5.7	0.19	0.17	29	26
MCM-41/TMB	9.0	9.1	7.8	7.6	11.9	0.63	1.08	33	56

MCM-41/TMB. These deviations may be explained by comparison of the equations used in TPM calculations. Equation (5) used in the case of heptane was proposed by Nedelec et al. [29] in a study on monolithic mesoporous silicas synthesized via sol–gel method. The authors assumed that the relation between ΔT and $1/R_p$ is linear. This assumption is questionable and the resulting simple form of the equation may explain greater uncertainty of the pore size for larger mesopores. On the other hand, Eq. (4) used for H_2O TPM proposed by Landry [4], taking into account nonlinear dependence of ΔT on $1/R_p$, better reproduces the PSDs in the studied silicas. In fact in the case of water TPM numerous studies have been performed, but choosing the right formula for determination of the pore size is quite complicated. It is not entirely clear why the results obtained by various groups are not in agreement [4, 16, 30–33]. Quite common is following the trend of linear dependence between ΔT on $1/R_p$, although non-linearity was empirically observed [4, 34]. For other probes, such as heptane, the literature reports are scarce, which makes attempts of application of the TPM method more difficult.

Conclusions

The results presented in this study demonstrate necessity of using complementary methods to study properties of porous materials. They also reveal a great potential of the TPM method based on observation of phase transitions of a liquid confined in the mesopores by means of DSC. This method seems to be especially suitable for study the porosity of the hydrated materials which can collapse during drying or for other samples which are difficult to be characterized with the conventional methods. Moreover, application of the TPM to solid materials may provided additional information about the samples or can be reasonable to calibration the other method for subsequent use.

The TPM measurements are relatively fast and highly reproducible. For uniform mesopores they give very narrow PSDs indicating high accuracy of the method. However, in order to improve precision of the method further research aimed at its development, especially with complementary use of water and various organic probes, seems necessary.

Acknowledgment The work of Maria Mańko was supported by the International PhD-studies programme at the Faculty of Chemistry Jagiellonian University within the Foundation for Polish Science MPD Programme co-financed by the EU European Regional Development Fund.

References

1. Davis ME. Ordered porous materials for emerging applications. Nature. 2002;417:813–21.
2. Riikonen J, Jarno Salonen J, Lehto V-P. Utilising thermoporometry to obtain new insights into nanostructured materials—review part 1. J Therm Anal Calorim. 2011;105(3):1811–21.
3. Iza M, Woerly S, Danumah C, Kaliaguine S, Bousmina M. Polymer. 2000;41:5885–93.
4. Landry M. Thermoporometry by differential scanning calorimetry: experimental considerations and applications. Thermochim Acta. 2005;433:27–50.
5. Ojeda M, Esparza J, Campero A, Cordero S, Kornhauser I, Rojas F. On comparing BJH and NLDFT pore-size distributions determined from N_2 sorption on SBA-15 substrata. Phys Chem Chem Phys. 2003;5:1859–66.
6. Allen T. Particle size measurement. New York: Chapman & Hall; 1997. p. 251.
7. Morishige K. Adsorption hysteresis in ordered mesoporous silicas. Adsorption. 2008;14(2–3):157–63.
8. Liu H, Zhang L, Seaton NA. Sorption hysteresis as a probe of pore structure. Langmuir. 1993;9(10):2576–82.
9. Groen JC, Peffer LAA, Pérez-Ramírez J. Pore size determination in modified micro- and mesoporous materials. Pitfalls and limitations in gas adsorption data analysis. Microporous Mesoporous Mater. 2003;60(1–3):1–17.
10. Makowski W. Quasi-equilibrated temperature programmed desorption and adsorption: a new method for determination of the isosteric adsorption heat. Thermochim Acta. 2007;454:26–32.
11. Makowski W, Ogorzałek Ł. Determination of the adsorption heat of *n*-hexane and *n*-heptane on zeolites beta, L, 5A, 13X, Y and ZSM-5 by means of quasi-equilibrated temperature-programmed desorption and adsorption (QE-TPDA). Thermochim Acta. 2007; 465:30–9.
12. Makowski W, Kuśtrowski P. Probing pore structure of microporous and mesoporous molecular sieves by quasi-equilibrated temperature programmed desorption and adsorption of *n*-nonane. Microporous Mesoporous Mater. 2007;102:283–9.
13. Makowski W, Chmielarz L, Kuśtrowski P. Determination of the pore size distribution of mesoporous silicas by means of quasi-equilibrated thermodesorption of *n*-nonane. Microporous Mesoporous Mater. 2009;120:257–62.
14. Thomson W. Phil Mag. 1871;42:448.
15. Billamboz N, Baba M, Grivet M, Nedelec J-M. A general law for predictive use of thermoporosimetry as a tool for the determination of textural properties of divided media. Phys Chem B. 2004;108:12032–7.
16. Brun M, Lallemand A, Quinson J, Eyraud C. A new method for the simultaneous determination of the size and shape of pores: the thermoporometry. Thermochim Acta. 1977;21:59–88.
17. Baba M, Nedelec J-M, Lacoste J. Porous volume of inorganic materials and degree of swelling of elastomers monitored by DSC measurements. J Phys Chem B. 2003;107:12884–90.
18. Kloetstra KR, Zandbergen HW, van Koten MA, van Bekkum H. Thermoporometry as a new tool in analyzing mesoporous MCM-41 materials. Catal Lett. 1995;33:145–56.
19. Yamamoto T, Endo A, Inagi Y, Ohmori T, Nakaiwa M. Evaluation of thermoporometry for characterization of mesoporous materials. J Colloid Interface Sci. 2005;284(2):614–20.
20. Baba M, Nedelec J-M, Lacoste J, Gardette J-L, Morel M. Crosslinking of elastomers resulting from ageing: use of thermoporosimetry to characterise the polymeric network with *n*-heptane as condensate. Polym Degrad Stab. 2003;80:305–13.
21. Mu R, Malhotra VM. Effects of surface and physical confinement on the phase transitions of cyclohexane in porous silica. Phys Rev B. 1991;44:4296–303.
22. Wulff M. Pore size determination by thermoporometry using acetonitrile. Thermochim Acta. 2004;419:291–4.
23. Galarneau A, Nader M, Guenneau F, Di Renzo F, Gedeon A. Understanding the stability in water of mesoporous SBA-15 and MCM-41. J Phys Chem C. 2007;111:8268–77.
24. Ottaviani MF, Moscatelli A, Desplantier-Giscard D, Di Renzo F, Kooyman PJ, Alonso B, Galarneau A. Synthesis of micelle-templated silicas from cetyltrimethylammonium bromide/1,3,5-trimethylbenzene micelles. J Phys Chem B. 2004;108:12123–9.
25. Di Renzo F, Testa F, Chem JD, Cambon H, Galarneau A, Plee D, Fajula F. Textural control of micelle-templated mesoporous silicates: the effects of co-surfactants and alkalinity. Microporous Mesoporous Mater. 1999;28:437–46.
26. Barrett EP, Joyner LG, Halenda PP. The determination of pore volume and area distributions in porous substances. I. Computations from nitrogen isotherms. J Am Chem Soc. 1951;73:373–80.
27. Jaroniec M, Solovyov LA. Improvement of the Kruk–Jaroniec–Sayari method for pore size analysis of ordered silicas with cylindrical mesopores. Langmuir. 2006;22:6757–60.
28. Riikonen J, Jarno Salonen J, Lehto V-P. Utilising thermoporometry to obtain new insights into nanostructured materials—review part 2. J Therm Anal Calorim. 2011;105(3):823–30.
29. Nedelec J-M, Baba M. On the use of monolithic sol–gel derived mesoporous silica for the calibration of thermoporisemetry using various solvents. J Sol Gel Sci Technol. 2004;31:169–73.
30. Ishikiriyama K, Todoki M. Evaluation of water in silica pores using differential scanning calorimetry. Thermochim Acta. 1995; 256:213–26.
31. Schreiber A, Ketelsen I, Findenegg GH. Melting and freezing of water in ordered mesoporous silica materials. Phys Chem Chem Phys. 2001;3:1185–95.
32. Ishikiriyama K, Todoki M, Motomura K. Pore size distribution (PSD) of silica gels by means of differential scanning calorimetry. J Colloid Interface Sci. 1995;171:92–102.
33. Schmidt R, Hansen EW, Stocker M, Akporiaye D, Ellestad OH. Pore size determination of MCM-41 mesoporous materials by means of 1H NMR spectroscopy, N_2 adsorption, and HREM. A preliminary study. JACS. 1995;117:4049–56.
34. Hansen EW, Gran HC, Sellevold EJ. Heat of fusion and surface tension of solids confined in porous materials derived from a combined use of NMR and calorimetry. J Phys Chem B. 1997; 101:7027–32.